Research

Authors for correspondence:
Chang Liu
e-mail: liu.chang1@ufl.edu
James M. Finley
e-mail: jmfinley@usc.edu

†Present address: Department of Biomedical Engineering, University of Florida, Gainesville, FL, USA.

Generalizability of foot placement control strategies during unperturbed and perturbed gait

Chang Liu[1,†], Francisco J. Valero-Cuevas[1,2,3] and James M. Finley[1,2,3]

[1]Department of Biomedical Engineering, [2]Division of Biokinesiology and Physical Therapy, and [3]Neuroscience Graduate Program, University of Southern California, Los Angeles, CA, USA

CL, 0000-0002-0381-4136; FJV-C, 0000-0002-2611-7923;
JMF, 0000-0003-2679-2221

Control of foot placement is an essential strategy for maintaining balance during walking. During unperturbed, steady-state walking, foot placement can be accurately described as a linear function of the body's centre of mass (CoM) state at midstance. However, it is uncertain if this mapping from CoM state to foot placement generalizes to larger perturbations that could potentially cause falls. Recovery from these perturbations may require reactive control strategies not observed during unperturbed walking. Here, we used unpredictable changes in treadmill belt speed to assess the generalizability of foot placement mappings identified during unperturbed walking. We found that foot placement mappings generalized poorly from unperturbed to perturbed walking and differed for forward perturbation versus backward perturbation. We also used the singular value decomposition of the mapping matrix to reveal that people were more sensitive to backward versus forward perturbations. Together, these results indicate that a single linear mapping cannot describe the foot placement control during both forward and backward losses of balance induced by treadmill belt speed perturbations. Better characterization of human balance control strategies could improve our understanding of why different neuromotor disorders result in heightened fall risk and inform the design of controllers for balance-assisting devices.

THE ROYAL SOCIETY
PUBLISHING

1. Introduction

Control of foot placement is an important strategy for maintaining balance during walking [1–4]. Balance can be controlled by adjusting the magnitude and orientation of ground reaction force vectors and their moment arm relative to the body's centre of mass (CoM) to influence the body's linear and angular momentum. While there are many strategies to stabilize the body during loss of balance, such as regulating lateral ankle roll or ankle push-off [3], modulating foot placement remains one of the primary strategies for controlling balance by varying the centre of pressure location and assisting in generating the ground reaction force needed to stabilize the body. For example, one way to recover from a forward loss of balance is to place the foot more anterior to the body's extrapolated CoM than normal. This strategy may produce a ground reaction force that has a greater posteriorly directed component to reduce forward linear momentum while also producing a backward moment about CoM to arrest the forward rotation of the body [5]. Thus, modulating foot placement from step to step is an important strategy for humans to maintain balance.

Step-to-step balance corrective strategies are often characterized using a data-driven approach relating foot placement location to the body's state at an earlier phase of the gait cycle [6–15]. Given an average CoM trajectory and many strides of steady walking, one can often derive a linear mapping between deviations of the CoM state from this trajectory to deviations in the next foot placement [8,11,12]. These mappings can explain approximately 80% of the variance in foot placement in the mediolateral direction and approximately 30 to 40% of the variance in the anteroposterior direction using the CoM state at midstance [12,13,16]. Though passive dynamics may lead to some degree of correlation between CoM state and foot placement [17], the high degree of variance explained, especially in the mediolateral direction, may indicate that the central nervous system uses information about the body's state to actively control the next foot placement during unperturbed walking.

Although the observed mappings explain foot placement patterns during unperturbed gait, the extent to which these mappings generalize to perturbed walking remains to be seen. It is conceivable that linear mappings may fail to explain balance-correcting responses to external perturbations because the neuromotor system is predominately nonlinear, especially during large perturbations [18]. If so, this would suggest that studying unperturbed walking alone is insufficient for elucidating the strategies that people use to prevent falls. While one previous study investigated the relationship between foot placement location and CoM state during perturbed walking [4], the authors used the body's state at foot strike rather than an earlier phase in the gait cycle. Additionally, this study did not examine the generality of the relationship from steady-state unperturbed gait to perturbed gait [4]. In addition, there is conflicting prior evidence regarding the generality of the relationship between CoM state and foot placement during different walking tasks. Joshi *et al*. [6] found that the mapping coefficients for unperturbed walking observed in [6] and [12] were similar to those observed in people who responded to small backward perturbations while walking. By contrast, Vlutters *et al*. [4] found that the mapping between the CoM state and foot placement differed for forward and backward perturbations. Therefore, it is possible that perturbation magnitude and direction explain the differences in the degree of generalizability observed across studies.

The primary goal of this study was to determine whether the mapping between CoM state and foot placement derived from unperturbed walking could explain the variance in foot placement in response to forward and backward perturbations in neurotypical adults. We hypothesized that a mapping which accounted for the directional differences in response to unexpected forward disturbance versus backward disturbance would better explain the variance in foot placement than a mapping derived solely from unperturbed walking. This is because one might expect different strategies to be effective when balance disturbances are in the same direction versus the opposite direction of both linear and angular momentum about the CoM [4]. Additionally, we performed singular value decomposition on the foot placement mapping to provide a direct assessment of the direction along which foot placement was most sensitive to deviations in CoM state and the sensitivity of foot placement control along that direction. We expected to find differences between unperturbed and perturbed walking in the derived foot placement mappings as well as the direction and sensitivity of foot placement control to deviations in CoM state. Overall, this study may extend our understanding of how people control foot placement to maintain balance during walking and may inform the design of controllers for assistive devices to stabilize walking in response to perturbations.

2. Material and methods

2.1. Participant characteristics

A total of 13 neurotypical adults with no musculoskeletal or gait impairments participated in this study (six female, 58 ± 29 years, 0.75 ± 0.25 m s^{-1}). These participants were recruited as age-matched controls for a sample of post-stroke participants from a prior study [5]. Exclusion criteria included any neurological, cardiovascular, orthopaedic and psychiatric diagnoses. All participants reported their right side as their dominant limb when asked which leg they would use to kick a ball. The study was approved by the Institutional Review Board at the University of Southern California (no. HS-18-00533), and all participants provided written informed consent before participating. All aspects of the study conformed to the principles described in the Declaration of Helsinki [19].

2.2. Experimental protocol

Participants walked on an instrumented, dual-belt treadmill (Fully Instrumented Treadmill, Bertec, Columbus, OH, USA) for six separate trials at their self-selected walking speed. We determined their self-selected walking speed using a two-alternative forced-choice staircase method [20–22] as described in [23]. Participants then walked on the treadmill for 5 min at their self-selected walking speed without receiving any perturbations. Then, for five subsequent trials, participants reacted to acceleration of the treadmill belts. Each trial consisted of a total of 24 perturbations, with 12 on each belt. The perturbations had magnitudes of −0.5, −0.4, −0.3, 0.3, 0.5 and 0.7 m s^{-1}, where positive values indicate increases in speed relative to the participant's self-selected walking speed, and negative values correspond to reductions in the participant's self-selected walking speed. We chose to use velocity to define perturbation magnitude for two reasons. First, belt velocity can be controlled more reliably than displacement or acceleration, and second, defining treadmill perturbations by velocity is consistent with what others have done in the literature [24,25]. Each perturbation was remotely triggered by customized MATLAB code, and the order of these perturbations was randomized. Each perturbation was characterized by a trapezoidal speed profile in which the ipsilateral treadmill belt accelerated at the time of foot strike to the target belt speed at an acceleration of 3 m s^{-2} (or −3 m s^{-2} if the target speed was less than their walking speed), held this speed for 0.7 s, and then returned to the participant's self-selected walking speed at an acceleration of −3 m s^{-2} (or 3 m s^{-2}) [26]. The perturbations were randomly triggered to occur within a range of 15–25 steps after the previous perturbation to provide participants with sufficient time to re-establish their baseline walking pattern and prevent them from anticipating perturbation timing.

2.3. Data acquisition

We used a 10-camera motion capture system (Qualisys AB, Gothenburg, Sweden) to record three-dimensional marker kinematics at 100 Hz and ground reaction forces at 1000 Hz. We placed a set of 14 mm spherical markers on anatomical landmarks and marker clusters on the upper arms, forearms, thighs, shanks and the back of the heels to create a 13-segment, full-body model [27,28]. We calibrated marker positions during a 5 s standing trial and removed all joint markers after the calibration.

2.4. Data processing

We post-processed the kinematic and kinetic data in Visual3D (C-Motion, Rockville, MD, USA) and Matlab 2020b (Mathworks, Natick, MA, USA) to compute variables of interest. We lowpass filtered marker positions and ground reaction forces using fourth-order Butterworth filters with cut-off frequencies of 6 and 20 Hz, respectively, based on previous literature [29–31]. Foot strike was defined as the time point when the vertical ground reaction forces reached 80 N. We chose to use an 80 N threshold to detect foot strikes because we used the same threshold to determine foot strikes in real time to elicit perturbations. During our study design, we found that an 80 N threshold was the minimum threshold to detect foot strikes with high accuracy in real time. We also examined the timing of perturbations relative to the foot strike post hoc to remove the perturbations that occurred more than 150 ms after the foot strike [32]. We included a median of 10 (interquartile range: 1) perturbations for each perturbation amplitude per side for each participant. On average, we removed

six perturbations out of 120 per participant. We also calculated the time between the subsequent foot strike after each perturbation and the onset of treadmill deceleration. The subsequent foot strike occurred before treadmill deceleration in over 97% of the perturbations.

2.5. Models of foot placement

Our goal was to derive a mapping between CoM state and foot placement to characterize the step-to-step balance corrective strategies during unperturbed and perturbed walking. We used the heel marker for the position of the foot. The CoM state during single limb stance, s, was defined as in equation (2.1):

$$s = [PCoM_{AP}, PCoM_{ML}, VCoM_{AP}, VCoM_{ML}]^T.$$ (2.1)

The position of the next foot placement q was defined as in equation (2.2)

$$q = [Foot_{AP}, Foot_{ML}]^T.$$ (2.2)

CoM state included the CoM position (PCoM) and velocity (VCoM) in the fore-aft (AP) and mediolateral (ML) direction. Both CoM state and foot placement positions were relative to the position of the current stance foot (figure 1). T represents the transpose of the matrix. We normalized position variables using the CoM height (H) of the participant and velocity variables using $\sqrt{gH}$, where g is the gravity constant [6]. Each step cycle was divided into 100 time points.

We defined the nominal trajectories of the CoM (s^*) and foot strike positions (q^*) as the average values of these quantities during unperturbed walking. Step-to-step fluctuations about the nominal trajectory allowed us to determine the relationship between deviations in foot positions $\Delta q = q_{k+1} - q^*$ and deviations in the CoM state $\Delta s = s_k - s^*$ (k is the step number). We derived the mapping between Δq and Δs at midstance, which was defined as 50% of the step cycle, to be consistent with previous studies and because it was early enough in the gait cycle to allow sufficient time for changes in foot placement by the swing limb [6,12,33]. We first estimated this relationship by computing the Jacobian matrix (**J**) during the step cycle that mapped the discrete change in state Δs to the change in foot position Δq equations (2.3) and (2.4). We assumed left–right symmetry so that the foot positions and the CoM state were mirrored about the sagittal plane [6,34].

$$\underset{2 \times 1}{\Delta q} \approx \underset{2 \times 4}{\mathbf{J}}\, \underset{4 \times 1}{\Delta s},$$ (2.3)

$$\underset{2 \times 4}{\mathbf{J}} = \begin{bmatrix} \dfrac{\partial Foot_{AP}}{\partial PCoM_{AP}} & \dfrac{\partial Foot_{AP}}{\partial PCoM_{ML}} & \dfrac{\partial Foot_{AP}}{\partial VCoM_{AP}} & \dfrac{\partial Foot_{AP}}{\partial VCoM_{ML}} \\ \dfrac{\partial Foot_{ML}}{\partial PCoM_{AP}} & \dfrac{\partial Foot_{ML}}{\partial PCoM_{ML}} & \dfrac{\partial Foot_{ML}}{\partial VCoM_{AP}} & \dfrac{\partial Foot_{ML}}{\partial VCoM_{ML}} \end{bmatrix} = \begin{bmatrix} \underset{1 \times 4}{\boldsymbol{j}_{AP}} \\ \underset{1 \times 4}{\boldsymbol{j}_{ML}} \end{bmatrix}$$ (2.4)

Given that **J** is not a full-rank matrix and maps from a higher (rank = 4) to a lower (rank = 2) dimension, it has a null space. The null space contains the set of vectors that define the directions along which deviations in CoM state would not affect foot placement. We further defined the first row of **J** matrix to be $\boldsymbol{j}_{AP}$ and the second row to be $\boldsymbol{j}_{ML}$ as they defined how deviations in CoM state influence foot placement in the anteroposterior direction and mediolateral direction, respectively.

2.6. Singular value decomposition of Jacobian matrix

The Jacobian matrix can be considered a form of a 'state transition matrix' that reflects the strength and direction of output responses (i.e. changes in foot placements) to inputs (i.e. changes in CoM state) in particular directions in this linearized analysis. The singular value decomposition of the Jacobian, therefore, can estimate the sensitivity of foot placement to changes in CoM state. Importantly, as the Jacobian matrix is not full rank, it maps from higher dimensional changes in CoM state to lower dimensional changes in foot placement. Singular value decomposition can thus determine the changes in CoM state that would produce no changes in foot placement (the null space of the Jacobian). Therefore, we performed singular value decomposition on $\boldsymbol{j}_{AP}$ and $\boldsymbol{j}_{ML}$ equation (2.5) to find their null spaces, determine in which direction the control of foot placement was the most sensitive to deviations
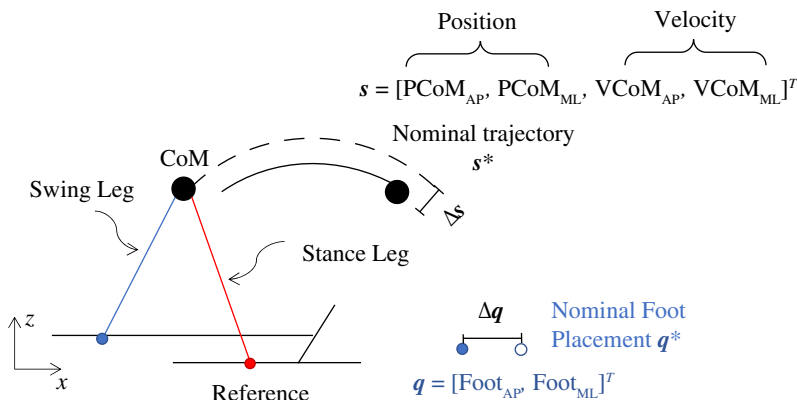
Figure 1. Diagram of the model describing the CoM state (s) and foot placement (q). CoM state included the CoM position (PCoM) and velocity (VCoM) in the fore-aft (anteroposterior, AP) and mediolateral (ML) direction. Blue: swing leg; red: stance leg. CoM position and the position of the swing foot were referenced to the stance foot. The black dashed trajectory represents the nominal (average) CoM trajectory. The black solid trajectory represents one measured trajectory. Δq and Δs represent the step-to-step fluctuation of the foot placement and CoM state.

in CoM state, and determine the sensitivity of foot placement control along that direction for each individual. Note that this direction does not represent the cardinal directions in physical space because it is a combination of both the position and velocity of CoM:

$$\underset{1 \times 4}{\boldsymbol{j}} = \underset{1 \times 1}{U} \underset{1 \times 4}{\boldsymbol{\Sigma}} \underset{4 \times 4}{\mathbf{V^T}}. \tag{2.5}$$

Here, the rank 1, 1×4 matrices $\boldsymbol{j}_{AP}$ and $\boldsymbol{j}_{ML}$ were decomposed as the product of a 1×1 matrix U, a 1×4 rectangular diagonal gain matrix $\boldsymbol{\Sigma}$ and a 4×4 orthogonal matrix $\mathbf{V}$, respectively. The first right singular vector of the Jacobian, $\boldsymbol{v_1}$, defined the direction along which foot placement was most sensitive to deviations in CoM state. The last three singular vectors ($\boldsymbol{v_2}$, $\boldsymbol{v_3}$ and $\boldsymbol{v_4}$) defined the null space directions along which deviations in CoM state would not affect the foot placement. The singular values of the gain matrix (Σ) indicated the sensitivity of foot placement to deviations in CoM state along the direction defined by $\boldsymbol{v_1}$.

2.7. Statistical analysis

Our objective was to determine whether the mapping between CoM state and subsequent foot placement differed between unperturbed and perturbed gait. We combined the data from all participants and used mixed-effects regression to determine the portion of the Jacobian that was consistent across participants (fixed effects) as well as random effects that account for the variability in elements of the Jacobian across participants. We did not find any collinearity among the independent variables for our models based on the variance inflation factor. We compared the ability of three models to explain anteroposterior and mediolateral foot positions during perturbed walking (table 1): (i) a linear model derived from unperturbed walking (model 1, equation (2.6)); (ii) a linear model derived from both perturbed steps and unperturbed steps (model 2, equation (2.7)), and (iii) a piecewise linear model derived from both perturbed steps and unperturbed steps (model 3, equation (2.8)). For models 2 and 3, we derived foot placement mappings using both the perturbed steps and an equal number of unperturbed steps because a prior study found that foot placement mapping coefficients for unperturbed and backward perturbed walking were similar [6]. Combining step types allowed us to identify a single mapping capable of explaining responses to both internally generated and external perturbations. We derived a piecewise linear mapping with one breakpoint (model 3,equation (2.8)) to test for directional differences in responses to increases and reductions in belt speed. We chose this piecewise linear model because there is evidence that people rely on different balance-correcting strategies to recover from forward loss of balance versus backward loss of balance [3,4,23,36].

We used the Akaike information criterion (AIC) to determine the most parsimonious model to explain variance in foot placement (equation (2.9)) [37]:

Table 1. Model description for foot placement mappings.

model description	model [35]	
linear mapping derived from unperturbed steps (model 1)	$\Delta \boldsymbol{q}_{k+1}^T = \mathbf{J}^1 \Delta \boldsymbol{s}_k^T$	(2.6)
linear mapping derived from both perturbed steps and unperturbed steps (model 2)	$\Delta \boldsymbol{q}_{k+1}^T = \mathbf{J}^2 \Delta \boldsymbol{s}_k^T$	(2.7)
a piecewise linear regression model derived from both perturbed steps and unperturbed steps (model 3)	$\Delta_{\boldsymbol{q}_{k+1}}^T = \begin{cases} \mathbf{J}^3 \Delta s_k^T & if\,\Delta \mathrm{VCoM}_{\mathrm{AP}} > 0 \\ \mathbf{J}^4 \Delta s_k^T & if\,\Delta \mathrm{VCoM}_{\mathrm{AP}} < 0 \end{cases}$	(2.8)

$$\mathtt{AIC} = 2k + N \ln \sum \varepsilon^2. \tag{2.9}$$

Here, k is the number of estimated parameters, N is the number of data points and ε is the prediction error between the predicted and actual data. We selected the model with the lowest AIC as the best model.

We also determined if the foot placement mapping differed between perturbed and unperturbed walking by comparing the regression coefficients of the foot placement mapping derived from perturbed walking and those derived from unperturbed walking. Finally, we determined whether the values of the gain matrix from singular value decomposition that indicated the sensitivity of foot placement control in response to deviations in CoM state differed between unperturbed walking and perturbed walking. We used a paired sample t-test if the variables were normally distributed; otherwise, we used the Wilcoxon rank-sum test. We used the Shapiro–Wilk test to test the normality. Significance was set at $p < 0.05$.

3. Results

3.1. Foot placement mapping during unperturbed walking

Both anteroposterior and mediolateral foot positions relative to the trailing limb varied from step to step during unperturbed walking (figure 2a, grey points). Foot position in the anteroposterior direction was explained by a model that included CoM displacement and velocity in both anteroposterior and mediolateral direction with the following form (mean ±s.e.), which had an R^2 of 0.38:

$$\boldsymbol{j}_{\mathrm{AP}}^{\mathbf{1}} = [0.71 \pm 0.088 \quad -0.81 \pm 0.12 \quad 0.77 \pm 0.088 \quad -0.94 \pm 0.13]. \tag{3.1}$$

Thus, a larger forward displacement of the CoM and larger forward velocity at midstance were associated with a longer step while a larger lateral CoM displacement and larger lateral velocity at midstance were associated with a shorter step. Foot position in the mediolateral direction was positively associated with CoM displacement and velocity in the mediolateral direction at midstance and negatively associated with CoM velocity in the anteroposterior direction, which had an R^2 of 0.74:

$$\boldsymbol{j}_{\mathrm{ML}}^{\mathbf{1}} = [-0.016 \pm 0.043 \quad 1.71 \pm 0.12 \quad -0.48 \pm 0.055 \quad 1.22 \pm 0.07]. \tag{3.2}$$

3.2. Foot placement mapping during perturbed walking

The mapping between foot position and CoM state at midstance during unperturbed waking did not generalize to foot positions following perturbations based on visual inspection of the predictions from the unperturbed model (figure 2). In both mediolateral and anteroposterior directions, we found that a piecewise linear model best explained the variance in foot placement as evidenced by the lower AIC values (table 2). Following forward perturbations, a larger forward displacement and larger forward velocity of the CoM at midstance were associated with a longer step, while a larger lateral CoM displacement and larger lateral velocity at midstance were associated with a shorter step:

$$\boldsymbol{j}_{\mathrm{AP}}^{\mathbf{3}} = [1.27 \pm 0.28 \quad -0.70 \pm 0.24 \quad 0.45 \pm 0.12 \quad -0.27 \pm 0.28]. \tag{3.3}$$
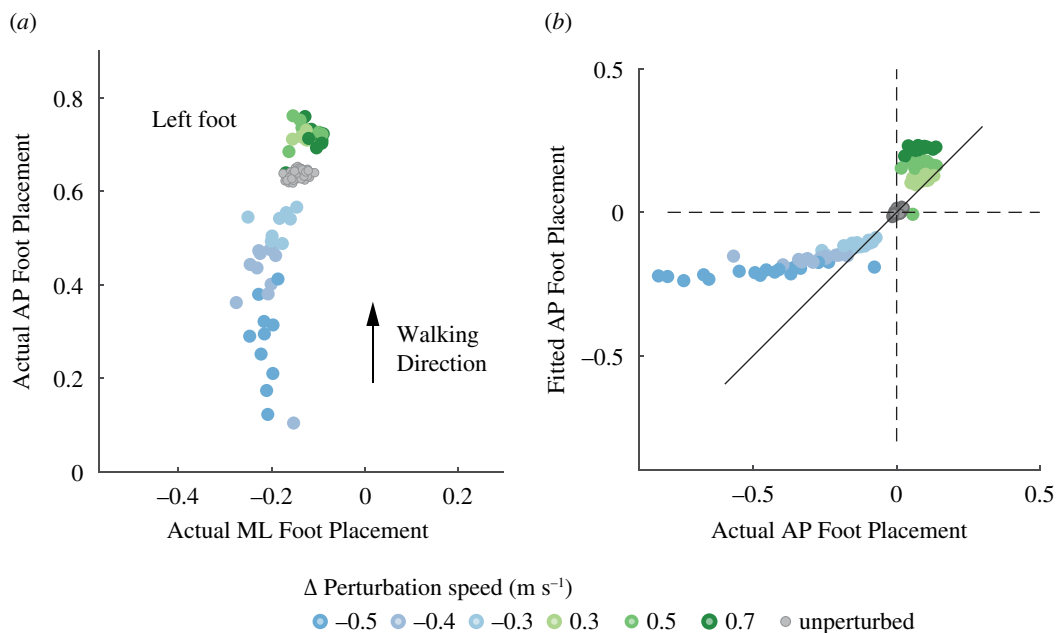
Figure 2. Scatter plots showing the left foot placement during unperturbed walking and following perturbations for a representative participant. Coloured dots indicate foot placement following increasing perturbations (blue to green). Grey dots represent foot placement during unperturbed walking. (*a*) Left foot placement relative to the right perturbed trailing stance foot during unperturbed steps and perturbed steps. (*b*) Actual foot placement versus fitted foot placement in the anteroposterior direction during both unperturbed and perturbed walking using the mapping derived from unperturbed steps.

Table 2. Model selection metrics based on AIC. Lower AIC values are indicative of better models.

model description	direction	number of estimated parameters (k)	AIC
linear mapping derived from unperturbed steps (model 1)	anteroposterior	9	12506
	mediolateral	9	5757
linear mapping derived from both perturbed steps and unperturbed steps (model 2)	anteroposterior	9	8364
	mediolateral	9	460
a piecewise linear model derived from both perturbed steps and unperturbed steps (model 3)	anteroposterior	18	6166
	mediolateral	18	−534

On the other hand, following backward perturbations, a larger backward displacement and larger backward velocity of CoM were associated with a shorter step while a larger lateral CoM displacement and larger medial velocity at midstance were associated with a shorter step:

$$\mathbf{j^4_{AP}} = [2.36 \pm 0.28 \quad -1.60 \pm 0.54 \quad 1.43 \pm 0.26 \quad 1.5 \pm 0.5]. \tag{3.4}$$

In the mediolateral direction, a larger lateral CoM velocity and displacement at midstance were associated with a wider step for both forward and backward perturbations. A larger forward CoM displacement and velocity were associated with a narrower step following forward perturbations. For backward perturbations, a larger backward CoM displacement and smaller backward CoM velocity were associated with a narrower step:

$$\mathbf{j^3_{ML}} = [-0.082 \pm 0.031 \quad 1.54 \pm 0.12 \quad -0.18 \pm 0.019 \quad 0.90 \pm 0.064], \tag{3.5}$$

$$\mathbf{j^4_{ML}} = [0.20 \pm 0.061 \quad 1.46 \pm 0.14 \quad -0.17 \pm 0.055 \quad 1.03 \pm 0.13]. \tag{3.6}$$

Several features of the anteroposterior foot placement mappings differed depending on the dataset for which they were derived (figure 3*a*). Coefficient estimates for each individual were computed
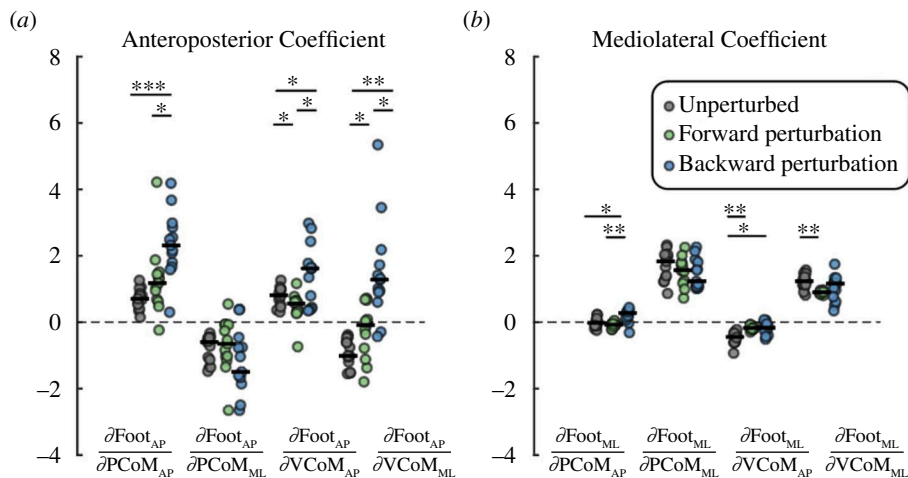
Figure 3. The estimated coefficients of the foot placement model in the anteroposterior direction (*a*), and mediolateral direction (*b*) with respect to CoM state at midstance. Coefficient estimates were computed by summing the random effects and the fixed effects from each mixed effect model. Black horizontal lines indicate the median coefficient estimates across participants. Grey: estimates from unperturbed walking (model 1); green: estimates from piecewise linear model for forward perturbations (model 3); blue: estimates from piecewise linear model for backward perturbations (model 3). Dots represent individual estimates of coefficients (*p < 0.05, **p < 0.001,***p < 0.0001).

by summing the random effects and the fixed effects from each mixed effect model. The coefficients for $\Delta PCoM_{AP}$ derived from backward perturbations were greater than those derived from forward perturbations (t_{12} = 4.3, p = 0.0011) and unperturbed walking (t_{12} = 5.6, p = 0.0001). Similarly, the coefficients for $\Delta VCoM_{AP}$ derived from backward perturbations were greater than those derived from forward perturbations (t_{12} = 2.4, p = 0.034) and unperturbed walking (t_{12} = 3.6, p = 0.0037). This suggests that, for a fixed magnitude deviation in CoM state, changes in foot placement were larger in response to backward perturbation versus forward perturbation. The coefficients for $\Delta VCoM_{ML}$ were greater when derived from forward perturbations than unperturbed walking (t_{12} = 3.5, p = 0.0043). The coefficients for $\Delta VCoM_{ML}$ derived from backward perturbations were also greater than those derived from forward perturbations (t_{12} = 3.1, p = 0.0093) and unperturbed walking (t_{12} = 5.0, p = 0.0003) and were generally positive while those derived from forward perturbations and unperturbed walking were generally negative. This suggests that a fixed magnitude of deviation in lateral CoM velocity would result in a longer step during backward perturbations but a shorter step during unperturbed walking and forward perturbations.

The mediolateral foot placement mapping derived from perturbed walking differed from that derived from unperturbed walking (figure 3*b*). The coefficients for $\Delta PCoM_{AP}$ derived from backward perturbations were higher than those from unperturbed walking (t_{12} = 3.82, p = 0.0024) and forward perturbations (t_{12} = 4.79, p = 0.0004). The coefficients for $\Delta VCoM_{AP}$ derived from unperturbed walking were more negative than those derived from forward perturbations (t_{12} = −5.3, p = 0.0002) and backward perturbations (t_{12} = −4.1, p = 0.0014). Finally, the coefficients for $\Delta VCoM_{ML}$ derived from forward perturbations were less than those derived from unperturbed walking (t_{12} = −5.3, p = 0.0002).

Although participants experienced many perturbations over the course of the experiment, we did not observe learning effects as measured by their responses to the perturbations. To assess the potential for learning, we compared the distance from the CoM to the rear edge of the base of support and also compared the CoM velocity in the anteroposterior direction at the time of foot strike after the first and last perturbations for each level of treadmill speed change [38]. There were no differences in these measures between the first and last perturbations (CoM position: p = 0.25; CoM velocity: p = 0.20), indicating that participants responded similarly to the perturbations throughout the experiment.
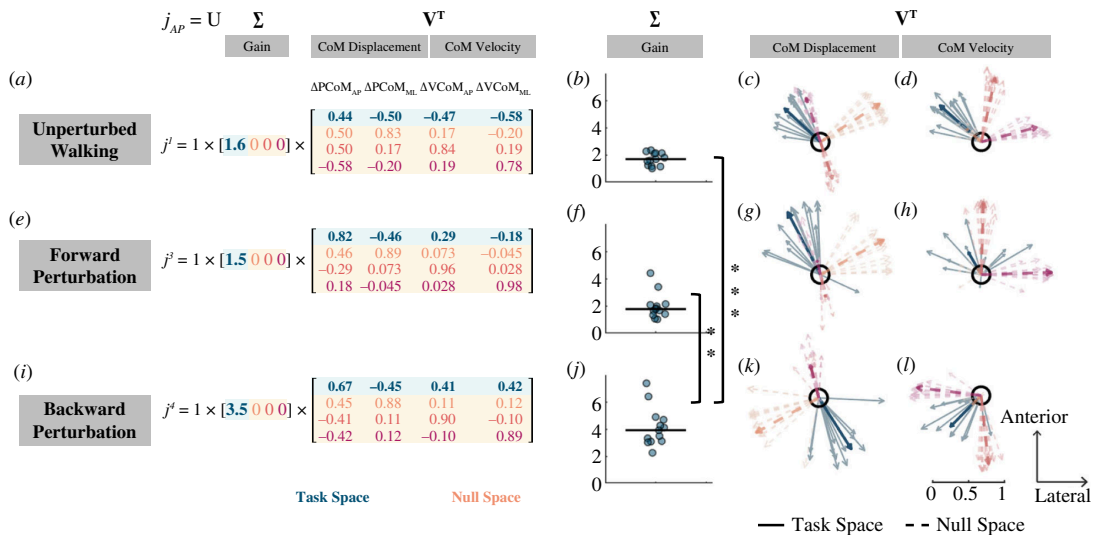
Figure 4. Visualization of singular value decomposition of the anteroposterior foot placement mapping matrix derived from unperturbed steps, forward perturbation and backward perturbation steps. The left panel shows singular value decomposition on the mean foot placement mapping matrix derived from unperturbed steps (*a*), forward perturbation (*e*), and backward perturbation steps (*i*). The gain obtained from singular value decomposition on the foot placement mapping for unperturbed steps (*b*), forward perturbation (*f*), and backward perturbations (*j*) for each individual (dot) and median across participants (black line) (**p < 0.001,***p < 0.0001). Right singular vectors related to ΔCoM displacement derived during steady-state walking (*c*), during forward perturbations (*g*), and during backward perturbations (*k*). Right singular vectors related to ΔCoM velocity derived from mapping coefficients during steady-state walking (*d*), during the forward loss of balance (*h*), and during the backward loss of balance (*l*). Light-coloured arrows indicate the right singular vectors for each individual. Note that solid arrows indicate the first right singular vector (task space vectors) while dashed lines indicate the last three singular vectors (null space vectors). Dark-coloured arrows indicate right singular vectors computed from the mean foot placement mapping matrix.

3.3. Singular value decomposition of foot placement mappings

3.3.1. Task space vectors for anteroposterior foot placement mapping matrix

Singular value decomposition provided a direct assessment of the null space of **J**, and the directions along which future foot placement $\Delta \boldsymbol{q}$ was the most sensitive to changes in CoM state $\Delta \boldsymbol{s}$ (figure 4*a–f* , blue arrows). We first performed singular value decomposition on the Jacobian matrix obtained for unperturbed walking $\boldsymbol{j}_{\mathbf{AP}}^{\mathbf{1}}$, forward perturbations $\boldsymbol{j}_{\mathbf{AP}}^{\mathbf{3}}$ and backward perturbations $\boldsymbol{j}_{\mathbf{AP}}^{\mathbf{4}}$ in the anteroposterior direction. During unperturbed walking ($\boldsymbol{j}_{\mathbf{AP}}^{\mathbf{1}}$), the largest foot placement changes were associated with deviations in CoM displacement and velocity that were directed anteriorly and medially (figure 4*a–d*). This was consistent with our interpretation in §3.1 that a larger forward displacement of the CoM and larger forward velocity at midstance were associated with a longer step, while a larger lateral CoM displacement and larger lateral velocity at midstance were associated with a shorter step. Following forward perturbations ($\boldsymbol{j}_{\mathbf{AP}}^{\mathbf{3}}$), people generally made the largest adjustment in foot placement in response to deviations in CoM displacement and velocity that were directed anteriorly and medially (figure 4*e–h*). However, it is important to note that there was large intersubject variability in response to deviations in CoM velocity in this case (figure 4*g*). Unlike the unperturbed and forward perturbation conditions, during the backward perturbations ($\boldsymbol{j}_{\mathbf{AP}}^{\mathbf{4}}$), the largest changes in foot placement were associated with posterior/lateral deviations of CoM displacement coupled with posterior/medial deviations in CoM velocity (figure 4*i–l*). The direction for deviations in CoM velocity was different from unperturbed steps and forward perturbations. Thus, these results suggest that changes in foot placement were direction-dependent in response to forward and backward perturbations in terms of CoM velocity, but the mapping remained relatively invariant in terms of CoM displacement.

3.3.2. Null space vectors for anteroposterior foot placement mapping matrix

Deviations in CoM state along the last three singular vectors (null space vectors) would not affect the foot placement. The orientations of null space vectors were similar for unperturbed walking and forward and backward perturbations. During both unperturbed and perturbed steps, deviations in CoM displacement in the anterior–lateral direction would not affect the anteroposterior foot placement position (figure 4, orange arrows). Deviations in CoM velocity directed anteriorly coupled with deviations in CoM displacement directed posteriorly would not affect anteroposterior foot placement position (figure 4, red arrows). Finally, deviations in CoM velocity directed laterally coupled with small deviations in CoM displacement in the anterior–medial direction would not affect foot placement position (figure 4, pink arrows).

3.3.3. Gain values for anteroposterior foot placement mapping matrix

Singular value decomposition of the anteroposterior foot placement mapping revealed higher control gain during backward perturbation than unperturbed walking and forward perturbation. The gain obtained for backward perturbations was higher than the gain obtained for unperturbed (Z = 4.2, p < 0.0001) and forward perturbation (p = 0.0003; figure 4b, f and j). These results indicated that foot placement was more sensitive to the changes in CoM state and may be more tightly controlled during backward perturbation than forward perturbation or unperturbed walking.

3.3.4. Task space vectors for mediolateral foot placement mapping matrix

Similarly, we performed singular value decomposition on the Jacobian matrix obtained for unperturbed walking j_{ML}^1, forward perturbations j_{ML}^3 and backward perturbations j_{ML}^4 in the mediolateral direction (figure 5). During both unperturbed walking and perturbed walking, a larger lateral displacement and velocity at midstance were associated with a wider step (figure 5, blue arrows). This was consistent with our results in §3.1 that a larger lateral displacement of the CoM and larger lateral velocity at midstance was associated with a longer step.

3.3.5. Null space vectors for mediolateral foot placement mapping matrix

The directions of null space vectors were similar for unperturbed walking and forward but not for backward perturbations. For unperturbed walking and forward perturbations, deviations in CoM displacement that were directed anteriorly and laterally did not affect foot placement position (figure 5c, d, g and h, orange arrows). Deviations in CoM velocity in the fore-aft direction also did not affect mediolateral foot placement position (figure 5c, d, g and h, red arrows). Deviations in CoM velocity directed laterally coupled with deviations in CoM displacement directed anteriorly and medially did not affect foot placement position (figure 5c, d, g and h, pink arrows). Following backward perturbations, deviations in CoM displacement that were directed posteriorly and medially did not affect foot placement position (figure 5k and l, orange arrows). Deviations in CoM velocity in the fore-aft direction also did not affect mediolateral foot placement position (figure 5k and l, red arrows). Deviations in CoM velocity directed laterally coupled with deviations in CoM displacement directed posteriorly and medially would not affect foot placement position (figure 5k and l, pink arrows).

3.3.6. Gain values for mediolateral foot placement mapping matrix

Finally, singular value decomposition on mediolateral foot placement mapping found similar gains during unperturbed walking, following forward and backward perturbations (p > 0.05; figure 5b, f and j). Such results indicated that the sensitivity of mediolateral foot placement to the changes in CoM state was similar during unperturbed walking and forward or backward perturbations.

4. Discussion

Our study's primary objective was to determine if the mapping between changes in CoM state and changes in foot placement found during steady-state, unperturbed walking explained changes in foot
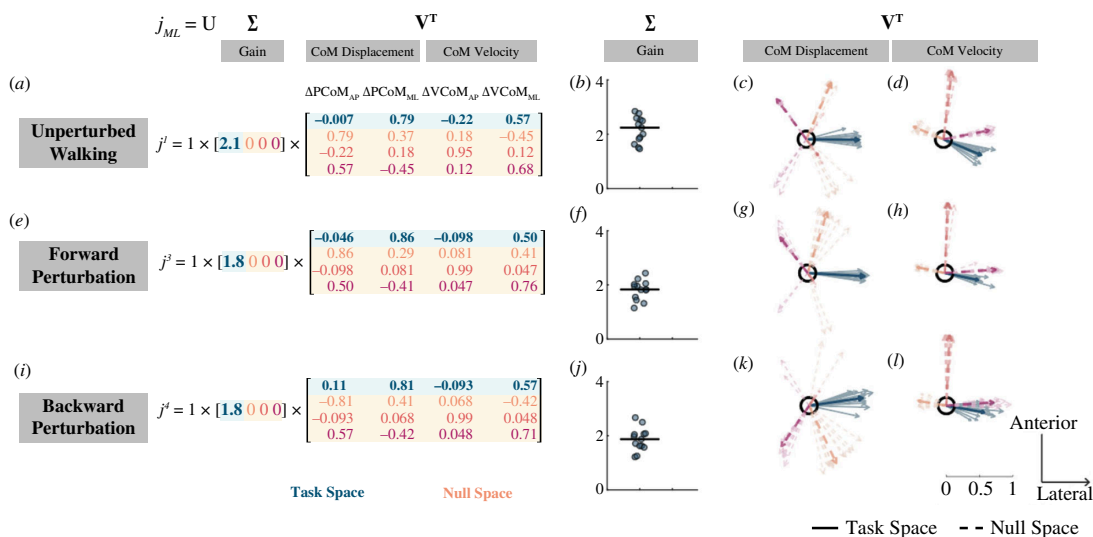
Figure 5. Visualization of singular value decomposition of the mediolateral foot placement mapping matrix derived from unperturbed steps, forward perturbation and backward perturbation steps. The left panel shows singular value decomposition on the mean foot placement mapping matrix derived from unperturbed steps (*a*), forward perturbation (*e*), and backward perturbation steps (*i*). The gain obtained from singular value decomposition on the foot placement mapping for unperturbed steps (*b*), forward perturbation (*f*), and backward perturbations (*j*) for each individual (dot) and median across participants (black line). Right singular vectors related to △CoM displacement derived during steady-state walking (*c*), during forward perturbation (*g*), and during backward perturbation (*k*). Right singular vectors related to △CoM velocity derived from mapping coefficients during steady-state walking (*d*), during the forward loss of balance (*h*), and during the backward loss of balance (*l*). Light-coloured arrows indicate the right singular vectors for each individual. Note that solid arrows indicate the first right singular vector (task space vectors) while dashed lines indicate the last three singular vectors (null space vectors). Dark-coloured arrows indicate right singular vectors computed from the mean foot placement mapping matrix.

placement in response to imposed perturbations. We found that the mapping derived from the natural variability of foot placement during steady-state walking could not explain patterns of foot placement in response to perturbations (figure 2*b*). Instead, a mapping that accounted for differences in responses to forward perturbation versus backward perturbation best-explained foot placement variance during perturbed steps (table 2). In addition, we found that foot placement was more sensitive to the changes in CoM state and more tightly correlated with backward perturbations than forward perturbations. Overall, our results demonstrate that a mapping which accounted for directional differences emerges when people adjust their foot placement in response to forward and backward perturbations.

The foot placement mapping during unperturbed walking in neurotypical participants was similar to that previously reported for young adults even though our population was, on average, older [12]. Our derived foot placement mappings explained approximately 60% of the variance in foot placement in the mediolateral direction and approximately 40% of the variance in the anteroposterior direction at midstance, which is comparable with prior work [12,16]. In the fore-aft direction, more lateral deviation of CoM displacement and CoM velocity at midstance was associated with a shorter step while a more forward deviation of CoM displacement and CoM velocity was associated with a longer step. In the mediolateral direction, more lateral deviation of CoM displacement and velocity was associated with a more lateral step. In both directions, people stepped in the direction of the CoM deviation. Such association between deviation in CoM state and foot placement could be attributed to passive dynamics of the swing leg and active control of foot placement to maintain balance [9,17]. Additionally, as in the neurotypical young population, the coefficient of determination at midstance was higher for mediolateral deviations in foot placement than fore-aft deviations, indicating that people may adopt a tighter control of their foot placement in the mediolateral direction than in the fore-aft direction.

We hypothesized that a mapping which accounted for the differences in response to forward disturbance versus backward disturbance would better explain the variance in foot placement than a linear mapping derived from unperturbed walking. Consistent with this hypothesis, we found that the foot placement mapping differed between forward versus backward perturbations. For instance, changes in foot placement in the anteroposterior direction were more sensitive to changes

in fore-aft CoM displacement and velocity at midstance following backward perturbations than forward perturbations. The discrepancy in foot placement mapping between forward and backward perturbations may result from the fact that people rely more on the modulation of ankle torque in the perturbed limb during forward perturbations than they do during backward perturbations [4,5]. Shifting the centre of pressure forward by activating the ankle plantar flexors during the stance phase in which forward perturbations occur could help people generate a backward moment about body CoM to reduce the forward rotation of the body. As a result, a smaller backward moment needs to be generated about the body's CoM at the next foot placement, and less foot placement deviation from the nominal trajectory was needed in response to forward perturbations than backward perturbations. It should be noted that the range of perturbation amplitudes differed for forward perturbation versus backward perturbation. Although we did not observe a difference in the foot placement mappings for large forward perturbation versus small forward perturbation, we cannot rule out the possibility that stepping responses to large backward perturbations (>0.5 m s^{-1}) may qualitatively differ from responses to smaller backward perturbations. Thus, future studies will need to assess the generalizability of our findings for large backward perturbations.

The mediolateral foot placement mapping derived from unperturbed walking also differed from the mapping derived from perturbed walking. Similar to what was observed with foot placement in the anteroposterior direction, these results indicate that the mapping between CoM state and foot placement observed during unperturbed walking does not generalize to perturbed walking. These results may indicate that our nervous system adjusts the control strategies following perturbations to generate appropriate corrective responses to maintain balance. This difference in control between steady-state and perturbed walking may reflect a shift from more spinally mediated control to control by brainstem or cortical circuits responsible for balance control [35,39,40]. For example, treadmill accelerations and decelerations which were similar to the perturbation paradigm used in this current study induced long-latency stretch reflexes in calf muscles that are thought to be mediated by supraspinal structures [41]. Therefore, analysis of unperturbed walking is insufficient to infer control strategies responsible for recovering from losses of balance.

The use of singular value decomposition extended our interpretations of foot placement control strategies beyond what could be inferred solely from the derived foot placement mappings. Performing singular value decomposition on the Jacobian matrix has been widely used for analysing and designing control systems [42]. In our analysis, we applied the decomposition to the experimental Jacobian matrices to obtain the direction along which changes in foot placement were most sensitive to changes in CoM state and the sensitivity (gain) along that direction. We found that both the direction and gain were similar for unperturbed steps and following forward perturbations. By contrast, the direction and gain were different following backward perturbations. This suggests that foot placement control strategies following backward perturbations were different from strategies during unperturbed and following forward perturbations. Particularly, the gain for backward perturbations was greater than unperturbed and forward perturbations, indicating higher sensitivity to deviations in CoM state following backward perturbations and, we speculate, tighter control of foot placement to correct for such deviations in CoM state compared to unperturbed and following forward perturbations.

Other stabilization strategies aside from foot placement, such as modulating the ankle push-off, also play an important role in maintaining balance [5,16,36,43,44]. We previously demonstrated that neurotypical participants coordinate both their leading and trailing limbs to restore balance in response to forward loss of balance [5]. Kim & Collins [33] derived a controller that used both foot placement and ankle push-off impulse to stabilize a biped in the sagittal plane when negotiating through random changes in the ground's height during walking. Therefore, future studies may investigate how different balance recovery strategies coordinate together following the deviation in the body's state and whether such coordination may explain the difference in foot placement mapping following the forward and backward perturbations.

Although we used CoM state as the predictor to derive the foot placement mapping, it is uncertain if CoM state provides the best predictive value. Other studies have used the swing leg state at the swing initiation [14], the stance leg state [13] or the ankle state [45] to construct predictive models that describe how humans control balance during walking or running. Future studies should perform a more comprehensive model comparison to determine the set of state variables best able to explain foot placement control during perturbed walking.

It also remains unclear to what extent passive dynamics versus active control contribute to the observed associations between CoM state and foot placement. For example, an open-loop stable two-dimensional model showed that 80% of the variance in foot position could be explained by CoM

state in the fore-aft direction at midstance [17]. One primary objective of our study was to derive the foot placement mapping during relatively large perturbations that required reactive control of balance to avoid falls. To our knowledge, no studies have examined the role of passive dynamics during balance corrections for perturbed walking. Given the inability of mappings derived from unperturbed walking to explain the variance in foot placement in the current study, this may suggest a larger contribution from active control in response to external perturbations. In addition, the previously examined two-dimensional bipedal model did not consider the inertial properties of the swing limb or consider control of the torso that helps to maintain an upright posture [17]. Thus, a more complex model with segment inertias [46] may be necessary to untangle the relative contribution of passive dynamics and active control to the correlation between the body's state and foot placement and draw inferences about how people use sensory feedback information to generate corrective responses.

It should be noted that the treadmill belt perturbations not only induced changes in the CoM dynamics but also induced changes in whole-body angular momentum [23]. Although peak whole-body angular momentum scales with perturbation amplitude [23], changes in whole-body angular momentum in response to treadmill perturbations do not correlate strongly with changes in foot placement [47]. This might be because recovery from changes in whole-body angular momentum in the sagittal plane is predominately achieved by changing the ground reaction force moment arm [5,48]. Thus, we feel that it is reasonable to omit changes in whole-body angular momentum when deriving models of foot placement control.

References

1. Bruijn SM, Meijer OG, Beek PJ, van Dieën JH. 2013 Assessing the stability of human locomotion: a review of current measures. *J. R. Soc. Interface* **10**, 20120999. (doi:10.1098/rsif.2012.0999)

2. Redfern MS, Schumann T. 1994 A model of foot placement during gait. *J. Biomech.* **27**, 1339–1346. (doi:10.1016/0021-9290(94)90043-4)

3. Reimann H, Fettrow T, Thompson ED, Jeka JJ. 2018 Neural control of balance during walking. *Front. Physiol.* **9**, 1271. (doi:10.3389/fphys.2018.01271)

4. Vlutters M, van Asseldonk EHF, van der Kooij H. 2016 Center of mass velocity-based predictions in balance recovery following pelvis perturbations during human walking. *J. Exp. Biol.* **219**, 1514–1523. (doi:10.1242/jeb.129338)

5. Liu C, McNitt-Gray JL, Finley JM. 2022 Impairments in the mechanical effectiveness of reactive balance control strategies during walking in people post-stroke. *Front Neurol.* **13**, 1032417. (doi:10.3389/fneur.2022.1032417)

6. Joshi V, Srinivasan M. 2019 A controller for walking derived from how humans recover from perturbations. *J. R. Soc. Interface* **16**, 20190027. (doi:10.1098/rsif.2019.0027)

7. Mahaki M, Bruijn SM, van Dieën JH. 2019 The effect of external lateral stabilization on the use of foot placement to control mediolateral stability in walking and running. *PeerJ* **7**, e7939. (doi:10.7717/peerj.7939)

8. Perry JA, Srinivasan M. 2017 Walking with wider steps changes foot placement control, increases kinematic variability and does not improve linear stability. *R. Soc. Open Sci.* **4**, 160627. (doi:10.1098/rsos.160627)

9. Rankin BL, Buffo SK, Dean JC. 2014 A neuromechanical strategy for mediolateral foot placement in walking humans. *J. Neurophysiol.* **112**, 374–383. (doi:10.1152/jn.00138.2014)

10. Roden-Reynolds DC, Walker MH, Wasserman CR, Dean JC. 2015 Hip proprioceptive feedback influences the control of mediolateral stability during human walking. *J. Neurophysiol*. **114**, 2220–2229. (doi:10.1152/jn.00551.2015)

11. Stimpson KH, Heitkamp LN, Horne JS, Dean JC. 2018 Effects of walking speed on the step-by-step control of step width. *J. Biomech*. **68**, 78–83. (doi:10.1016/j.jbiomech.2017.12.026)

12. Wang Y, Srinivasan M. 2014 Stepping in the direction of the fall: the next foot placement can be predicted from current upper body state in steady-state walking. *Biol. Lett*. **10**, 20140405. (doi:10.1098/rsbl.2014.0405)

13. Arvin M, Hoozemans MJM, Pijnappels M, Duysens J, Verschueren SM, van Dieën JH. 2018 Where to step? Contributions of stance leg muscle spindle afference to planning of mediolateral foot placement for balance control in young and old adults. *Front. Physiol*. **9**, 1134. (doi:10.3389/fphys.2018.01134)

14. Dean JC, Kautz SA. 2015 Foot placement control and gait instability among people with stroke. *J. Rehabil. Res. Dev*. **52**, 577–590. (doi:10.1682/JRRD.2014.09.0207)

15. Seethapathi N, Srinivasan M. 2019 Step-to-step variations in human running reveal how humans run without falling. *Elife* **8**, 1–24. (doi:10.7554/eLife.38371)

16. Jin J, van Dieën JH, Kistemaker D, Daffertshofer A, Bruijn SM. 2023 Does ankle push-off correct for errors in anterior-posterior foot placement relative to center-of-mass states? *PeerJ* **11**, e15375. (doi:10.7717/peerj.15375)

17. Patil NS, Dingwell JB, Cusumano JP. 2019 Correlations of pelvis state to foot placement do not imply within-step active control. *J. Biomech*. **97**, 109375. (doi:10.1016/j.jbiomech.2019.109375)

18. Khoo MCK. 2018 Physiological control systems. In 10. in: Nonlinear analysis of physiological control systems, pp. 317–376. Hoboken, NJ: John Wiley & Sons, Ltd. See https://onlinelibrary.wiley.com/doi/book/10.1002/9781119058786. (doi:10.1002/9781119058786)

19. World Medical Association. 2013 World Medical Association Declaration of Helsinki: ethical principles for medical research involving human subjects. *J. Am. Med. Assoc*. **310**, 2191–2194. (doi:10.1001/jama.2013.281053)

20. Dal U, Erdogan T, Resitoglu B, Beydagi H. 2010 Determination of preferred walking speed on treadmill may lead to high oxygen cost on treadmill walking. *Gait Posture* **31**, 366–369. (doi:10.1016/j.gaitpost.2010.01.006)

21. Farrens AJ, Lilley M, Sergi F. 2020 Training propulsion via acceleration of the trailing limb. *IEEE Trans. Neural. Syst. Rehabil. Eng*. **28**, 2816–2825. (doi:10.1109/TNSRE.2020.3032094)

22. García-Pérez MA. 1998 Forced-choice staircases with fixed step sizes: asymptotic and small-sample properties. *Vision Res*. **38**, 1861–1881. (doi:10.1016/s0042-6989(97)00340-4)

23. Liu C, Park S, Finley J. 2022 The choice of reference point for computing sagittal plane angular momentum affects inferences about dynamic balance. *PeerJ* **10**, e13371. (doi:10.7717/peerj.13371)

24. Martelli D, Monaco V, Bassi Luciani L, Micera S. 2013 Angular momentum during unexpected multidirectional perturbations delivered while walking. *IEEE Trans. Biomed. Eng*. **60**, 1785–1795. (doi:10.1109/TBME.2013.2241434)

25. Liss DJ, Carey HD, Yakovenko S, Allen JL. 2022 Young adults perceive small disturbances to their walking balance even when distracted. *Gait Posture* **91**, 198–204. (doi:10.1016/j.gaitpost.2021.10.019)

26. Liu C, Macedo LD, Finley JM. 2018 Conservation of reactive stabilization strategies in the presence of step length asymmetries during walking. *Front. Hum. Neurosci*. **12**, 251. (doi:10.3389/fnhum.2018.00251)

27. Havens KL, Mukherjee T, Finley JM. 2018 Analysis of biases in dynamic margins of stability introduced by the use of simplified center of mass estimates during walking and turning. *Gait Posture* **59**, 162–167. (doi:10.1016/j.gaitpost.2017.10.002)

28. Song J, Sigward S, Fisher B, Salem GJ. 2012 Altered dynamic postural control during step turning in persons with early-stage Parkinson's disease. *Parkinsons Dis*. **2012**, 386962. (doi:10.1155/2012/386962)

29. Kurz MJ, Arpin DJ, Corr B. 2012 Differences in the dynamic gait stability of children with cerebral palsy and typically developing children. *Gait Posture* **36**, 600–604. (doi:10.1016/j.gaitpost.2012.05.029)

30. Reisman DS, Wityk R, Silver K, Bastian AJ, Manuscript A. 2009 Split-belt treadmill adaptation transfers to overground walking in persons poststroke. *Phys. Ther*. **23**, 735–744. (doi:10.1177/1545968309332880.Split-Belt)

31. Winter DA. 2009 *Biomechanics and motor control of human movement*. Hoboken, NJ: John Wiley & Sons. See https://onlinelibrary.wiley.com/doi/book/10.1002/9780470549148

32. Buurke TJW, Liu C, Park S, den Otter R, Finley JM. 2020 Maintaining sagittal plane balance compromises frontal plane balance during reactive stepping in people post-stroke. *Clin. Biomech*. **80**, 105135. (doi:10.1016/j.clinbiomech.2020.105135)

33. Kim M, Collins SH. Once-per-step control of ankle push-off work improves balance in a three-dimensional simulation of bipedal walking. *IEEE Trans. Robot*. **33**, 406–418. (doi:10.1109/TRO.2016.2636297)

34. Ankaralı MM, Sefati S, Madhav MS, Long A, Bastian AJ, Cowan NJ. 2015 Walking dynamics are symmetric (enough). *J. R. Soc. Interface* **12**, 20150209. (doi:10.1098/rsif.2015.0209)

35. Solopova IA, Kazennikov OV, Deniskina NB, Levik YS, Ivanenko YP. 2003 Postural instability enhances motor responses to transcranial magnetic stimulation in humans. *Neurosci. Lett*. **337**, 25–28. (doi:10.1016/s0304-3940(02)01297-1)

36. Pijnappels M, Bobbert MF, van Dieën JH. 2005 Push-off reactions in recovery after tripping discriminate young subjects, older non-fallers and older fallers. *Gait Posture* **21**, 388–394. (doi:10.1016/j.gaitpost.2004.04.009)

37. Akaike H. 1981 Likelihood of a model and information criteria. *J. Econ*. **16**, 3–14. (doi:10.1016/0304-4076(81)90071-3)

38. Wang TY, Bhatt T, Yang F, Pai YCC. 2012 Adaptive control reduces trip-induced forward gait instability among young adults. *J. Biomech*. **45**, 1169–1175. (doi:10.1016/j.jbiomech.2012.02.001)

39. Deliagina TG, Orlovsky GN, Zelenin PV, Beloozerova IN. 2006 Neural bases of postural control. *Physiology* **21**, 216–225. (doi:10.1152/physiol.00001.2006)

40. Finley JM, Dhaher YY, Perreault EJ. 2013 Acceleration dependence and task-specific modulation of short- and medium-latency reflexes in the ankle extensors. *Physiol. Rep*. **1**, e00051. (doi:10.1002/phy2.51)

41. Sloot LH, van den Noort JC, van der Krogt MM, Bruijn SM, Harlaar J. 2015 Can Treadmill Perturbations Evoke Stretch Reflexes in the Calf Muscles? *PLoS One* **10**, e0144815. (doi:10.1371/journal.pone.0144815)

42. Klema V, Laub A. 1980 The singular value decomposition: its computation and some applications. *IEEE Trans. Automat. Contr*. **25**, 164–176. (doi:10.1109/TAC.1980.1102314)

43. Afschrift M, De Groote F, Jonkers I. 2021 Similar sensorimotor transformations control balance during standing and walking. *PLoS Comput. Biol*. **17**, e1008369. (doi:10.1371/journal.pcbi.1008369)

44. Rafiee S, Kiemel T. 2020 Multiple strategies to correct errors in foot placement and control speed in human walking. *Exp. Brain Res*. **238**, 2947–2963. (doi:10.1007/s00221-020-05949-x)

45. Maus HM, Revzen S, Guckenheimer J, Ludwig C, Reger J, Seyfarth A. 2015 Constructing predictive models of human running. *J. R. Soc. Interface* **12**, 103. (doi:10.1098/rsif.2014.0899)

46. Nozari P, Finley JM. Development of a platform to evaluate principles of bipedal locomotion using dynamical movement primitives. In *Int. IEEE/EMBS Conf. on Neural Engineering, NER. vol. 2019-March*, pp. 1062–1065. San Francisco, CA, USA: IEEE Computer Society.

47. Leestma JK, Golyski PR, Smith CR, Sawicki GS, Young AJ. 2023 Linking whole-body angular momentum and step placement during perturbed human walking. *J. Exp. Biol*. **226**, jeb244760. (doi:10.1242/jeb.244760)

48. van Mierlo M, Ambrosius JI, Vlutters M, van Asseldonk EHF, van der Kooij H. 2022 Recovery from sagittal-plane whole body angular momentum perturbations during walking. *J. Biomech*. **141**, 111169. (doi:10.1016/j.jbiomech.2022.111169)

49. OSF. 2023 Data from: Generalizability of foot-placement control strategies during unperturbed and perturbed gait. *OSF*. https://osf.io/gv5tq/?view_only=858243326d374cd3ba6ddd157195d02f